22 Myr-climate history recorded in the eolian deposits in China

Z.T. Guo[1,2], Q.Z. Hao[2], J.J. Wei[2], S.Z. Peng[2], Z.S. An[1] & T.S. Liu[1,2]

1. Institute of Earth Environment, Chinese Academy of Sciences, P.O. Box 17, Xi'an 710075, China
2. Institute of Geology and Geophysics, Chinese Academy of Sciences, P.O. Box 9825, Beijing 100029, China

1. A 22-Myr eolian history in northern China

The history of eolian dust deposition in northern China has been traced back to 22 Myr (Guo et al., 2002). Eolian deposits include the well-known loess-soil sequences of the last 2.6 Myr (Fig. 1a), containing more than fifty loess and soil layers, the Hipparion Red-Earth, also referred to as Red-Clay (2.6-8.0 Myr) of eolian origin in the eastern Loess Plateau (Fig. 1b) and the Miocene-Pliocene loess-soil sequences (3.5-7.1 Myr, Fig. 1c) and the Miocene loess-soil sequences (6.2-22 Myr, Fig. 1d) in the western Loess Plateau that contain several hundred pairs of loess/soil layers. The combination of these eolian formations provides a nearly continuous terrestrial climate record since the early Neogene.

Fig. 1a A picture of a loess-soil sequence of the last 2.6 Myr in Shaanxi (Details of loess of this age in Liu et al.,1985;An et al., 1990)

Fig 1b *Hipparion* Red-Earth (Red Clay, 2.6-8 Myr) at Xifeng (Details in Guo et al., 2001; 2004)

Fig 1c A loess-soil sequence of late Miocene-Pliocene age (3.5-7.1 Myr) at Dongwan in the western Loess Plateau (Hao and Guo, 2004)

Fig. 1d A Miocene loess-soil sequence (QA-I) at Qinan dated by geomagnetic method and micro-mammalian fossils for 6.2-22 Myr (Guo et al., 2002)

2. Evidence of eolian origin of the Miocene sequences

The Qinan region was characterized by two distinct tectonic/sedimentary settings, i.e. the plateau setting where Miocene loess-soil sequences were developed, and the basin setting where waterlain deposits were developed (Fig. 2). The eolian origin of these sequences is evidenced by (1) the presence of several hundred of paleosols (Fig. 1d and 3a), as confirmed by micro-morphological studies (Fig. 3b and 3c) interbedded with loess-layers with the lateral occurrences following the fluctuations of paleo-topographic surfaces (Fig. 4); (2) the similarity of quartz grain morphology (Fig. 3d), geochemical properties and grain-size distributions (Fig. 3e-h) to those of the Quaternary loess; (3) the variations of grain-size along the sequences (Fig. 5) characteristics of eolian deposits; (4) the presence of terrestrial mollusks along the sequences and the lack of aquatic species (Fig. 6, Li et al., 2005); (5) the spatially correlative magneto- and litho-stratigraphy, magnetic susceptibility and grain-size timeseries (Fig. 7) (see also Liu et al., 2005), and (6) the cyclical changes of various climate proxies along the sequences (Fig. 8), similar to these recorded by Quaternary loess-soil sequences. Pollen analyses indicate more humid conditions for soils layers and drier conditions for loess layers (Fig. 9).

Fig. 2 Tectonic/sedimentary settings of the Qinan Miocene loess deposits (according to Ma et al., 1989). The QA-I and QA-II sites are located within a plateau (a compressional ridge).

Fig. 3a, Field picture showing the alternation of loess and paleosols in QA-I. **b**, Microscopic image showing the groundmass of a paleosol. **c**, Microscopic image showing the clay coatings in paleosols. **d**, Angular morphology of quartz grains under scanning electronic microscope.

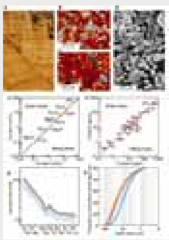

e-g, Comparison of major trace and rare earth element compositions between the Qinan eolian deposits and Quaternary loess from Xifeng. **h**, Grain-size distributions of the Qinan eolian deposits (blue lines) and the Quaternary Xifeng loess (red lines).

Fig.4 Lateral occurrences of loess and soil layers in QA-II following the fluctuations of paleo-topographic surfaces, feature typical of eolian sequence under subaerial conditions.

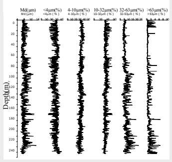

Fig.5 Grain-size analyses from QA-I based on 2531 samples showing the texture of the sequence is characteristic of eolian deposits. The fraction >63 μm represents less than 6.5%, with the maximum particle size mostly less than 120 μm. The median grain-size (Md) varies from ~6 to ~14 μm within a ~16 million-year time span.

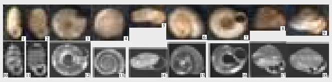

Fig. 6 Comparison between the land snails from a Qinan eolian sequence (upper range) and those from the Quaternary loess (lower range)

1, 10 *Gastrocopta armigerella*; 2, 11 *Pupilla aeoli*; 3, 12 *Punctum orphana*; 4, 13 *Punctum orphana*; 5, 14 *Punctum orphana*; 6, 15 *Vallonia*; 7, 16 *Vallonia*; 8, 17 *Metodontia beresowskii*; 9, 18 *Metodontia huaiensis*

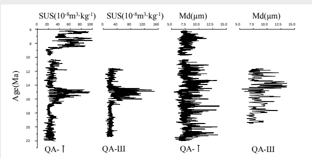

Fig.7 Comparative variations of magnetic susceptibility (SUS) and median grain-size (Md) between QA-I and QA-III (30 km east to QA-I). The spatially correlative stratigraphy, susceptibility and grain-size timeseries are characteristic of eolian deposits.

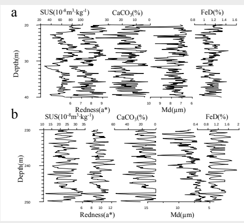

Fig. 8 Variations of magnetic susceptibility, Redness, $CaCO_3$ content, median grain-size (Md) and Free iron oxides (FeD) in QA-I (20-40 m and 230-250 m portions as examples). Soil layers are characterized by finer grain-size, higher susceptibility and FeD, lower $CaCO_3$ content compared with the surrounding loess layers. These fluctuation patterns are highly similar to those of the Quaternary loess-soil sequences although the dominant periods are different.

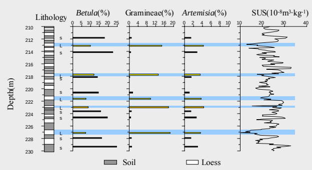

Fig. 9 Pollen assemblages from representative soil and loess layers in QA-I, showing much drier conditions for loess layers than for soil layers.

3. Continental climate changes from over-orbital to millennial scales

At over-orbital scale, the 22-Myr eolian deposits documented the aridity changes in the Asian inlands (Fig. 10). The onset of loess-soil formation by 22 Myr indicates the existence of sizeable inland deserts in Asia as dust sources, a energetic winter monsoon as dust carrier and a summer monsoon as a supply of moisture. From 22 to 6 Myr, evolution of the aridity was not strongly correlative with the global cooling trends (Fig. 10). However, the drying history since 6 Myr matches the ongoing high-latitude cooling and the consequent expansion of Arctic ice (Fig. 11 and 12). Some events also coincide with proposed uplift of portions of the Tibetan Plateau. At the orbital scales, the Miocene loess-soil sequence documented climate changes at Milankovitch frequencies (Fig. 13). Pliocene changes were dominated by ~41 ka cycles, consistent with the marine records (Fig. 14). Most of the Quaternary proxies yield frequency patterns essentially similar to that of the marine record (Fig. 15). Chemical weathering of loess also shows millennial changes of the summer monsoon correlative with those in the circum-North Atlantic region (Fig. 16).

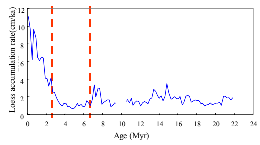

Fig. 10 Aridity evolution in the dust source areas as reflected by loess accumulation rate for the past 22 Myr. The Miocene was characterized by moderate levels of aridity and winter monsoon strength. Drastic increase in the aridity occurred at ~3.6 Myr. Data for 22-6.2 Myr are from the Qinan QA-I sequence (Guo et al., 2002). The interruption around 10 Myr corresponds to an hiatus. Data for 6.2-2.6 Myr are from the Xifeng *Hipparian* Red-Earth (Guo et al., 2001) and data for 0-2.6 Myr are from the Xifeng loess-soil sequence (Guo et al., 2004).

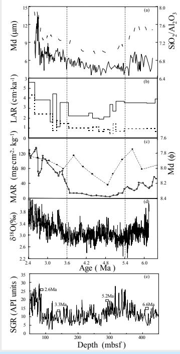

Fig. 11 Figure showing consistent changes between the aridity in the Asian interior and the global cooling trends from 6.2 to 2.6 Myr. (a) Variations of median grain-size (solid line) and the SiO_2/Al_2O_3 molecular ratio (a proxy of original eolian grain-size, dashed line) versus age. (b) Linear accumulation rates of the Xifeng (dashed line, after Sun et al., 1998) and Lingtai (solid line, after Ding et al., 1998) Red-Earth sequences. (c) Mass accumulation rate (MAR, solid line) and eolian grain-size (dotted line) from the North Pacific ODP Site 885/886 (Rea et al., 1998). (d) Marine d18O record from ODP Site 846 (Shackleton et al., 1995). (e) Natural gamma radioactivity plotted against depth with age controls. It is a measure of ice-rafted terrigenous detrital sediment content at the ODP Site 883 (DeMenocal, 1993).

Fig. 12 Coupled changes between the loess accumulation rate in the central Loess Plateau (Xifeng, thick line) and the marine d18O record (fine line). The composite marine d18O sequence shown here is a 20-point moving average curve based on the data from V19-30 (Shackleton and Pisias, 1985), ODP 677 (Shackleton et al., 1990) and ODP 846 sites (Shackleton et al., 1995).

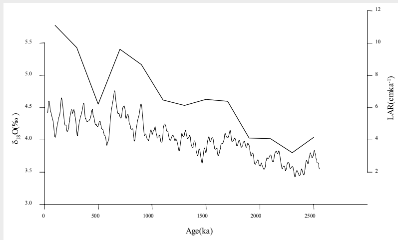

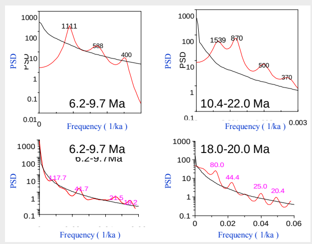

Fig. 13 Spectral analyses of the magnetic susceptibility timeseries for representative intervals from QA-I. Analyses were made using the Maximum entropy method.

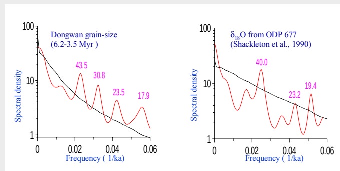

Fig. 14 Spectral analyses of the grain-size timeseries from Dongwan using the Maximum entropy method, showing Loess deposition and soil formation at astronomical frequencies during late Miocene and Pliocene times (3.5-6.2 Ma)

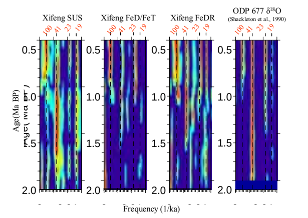

Fig. 15 Maximum entropy spectral analyses for magnetic susceptibility, FeD/FeT or FeDR (proxies of pedogenic intensity) from the loess-soil sequence of the last 2.6 Myr at Xifeng. The spectral patterns are essentially similar to those of marine $\delta^{18}O$ (ice-volume changes). Climate changes are characterized by dominant 40-kyr obliquity cycles during the 2.6-1.0 Myr and dominant 100-kyr eccentricity cycles during the last 1.0 Myr

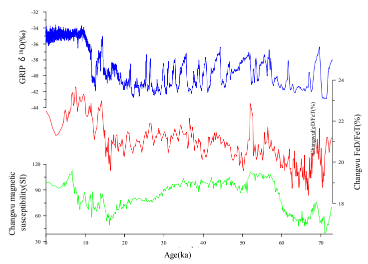

Fig. 16. Comparison of the GRIP d18O record (Dansgaard et al., 1993) with FeD/FeT ratios (a high-resolution paleoweathering record analyzed at 2.5 cm intervals) and magnetic susceptibility of the Changwu loess-soil sequence (central Loess Plateau) of the last 73 ka (the FeD/FeT timeseries is a 3-point moving average curve). The FeD/FeT ratio primarily reflects changes in the East-Asian summer monsoon.Over the last glacial period, general agreement can be observed between the loess weathering record and the GRIP ice d18O record.

Main references related to the contents

1. Guo Z T, Peng S Z, Hao Q Z, Biscaye P E, Liu D S, 2001. Origin of the Miocene-Pliocene red-earth formation at Xifeng in Northern China and implications for paleoenvironments. *Palaeogeography, Palaeoclimatology, Palaeoecology*, 170: 11-26.
2. Guo Z T, Ruddiman W F, Hao Q Z, Wu H B, Qiao Y S, Zhu R X, Peng S Z,Wei J J, Yuan B Y, Liu T S. 2002, Onset of Asian desertification by 22 Myr ago inferred from loess deposits in China. *Nature*, 416:159-163.
3. Guo, Z.T., Peng, S.Z., Hao, Q.Z., Biscaye, P. E., An, Z.S. and Liu, T.S., 2004, Late Miocene-Pliocene development of Asian aridification as recorded in an eolian sequence in northern China. *Global and Planetary Changes* 41(3-4): 135-145.
4. Guo, Z.T., Hao, Q.Z., Wei, J.J. and An, Z.S., 2005, Astronomical signals in different climate proxies from the Quaternary loess-soil sequences in China. Proceedings of Milutin Milankovitch Anniversary Symposium: Paleoclimate and the Earth Climate System (in press).
5. Hao, Q.Z. and Guo Z.T. 2004, Magnetostratigraphy of a late Miocene-Pliocene loess-soil sequence in the western Loess Plateau in China. *Geophysical Research Letters* 31:L09209.
6. Li, F.J., Wu, N.Q., Pei, Y.P. and Hao, Q.Z., 2005, Terrestrial mollusk evidence for the origin of a late Tertiary loess-paleosol sequence at Qinan in the western Chinese loess plateau, *Quaternary Sciences*, 25: 510~515.
7. Liu, J. F., Guo, Z.T., Hao, Q. Z., Peng, S.Z., Qiao, Y.S., Sun, B. and Yuan, B.Y., 2005, Magetostratrigraphy of the Miziwan Miocene eolian deposits in Qinan Country (Gansu Province), *Quaternary Sciences*, 25(4): 503~509.
8. Liu, J.F., Guo, Z.T., Qiao, Y.S., Hao, Q.Z. and Yuan, B.Y. 2005, Eolian origin of the Miocene loess-soil sequence at Qinan, China: evidence of Quartz morphology and Quartz grain-size. *Chinese Science Bulletin* (in press).

Correspondence: Guo Zhengtang, ztguo@mail.iggcas.ac.cn